Supporting information for:

Mechanism of Vanadium Leaching During Surface Weathering of

Basic Oxygen Furnace Steel Slag Blocks: A μXANES and SEM Study

Andrew J. Hobson[1], Douglas I. Stewart[2], Andrew W. Bray[1], Robert J. G. Mortimer[3], William M. Mayes[4], Michael Rogerson[4] and Ian T. Burke[1]

[1]School of Earth and Environment, University of Leeds, Leeds, LS2 9JT, UK.

[2]School of Civil Engineering, University of Leeds, Leeds, LS2 9JT, UK.

[3]School of Animal, Rural and Environmental Sciences, Nottingham Trent University, Brackenhurst Campus, Southwell, Nottinghamshire NG25 0QF, UK

[4]School of Environmental Sciences, University of Hull, Hull, HU6 7RX, UK.

Email for correspondence: i.t.burke@leeds.ac.uk, phone: +44 113 3437532, fax: +44 113 3435259

Section S1. SEM analysis.

In order to prepare the samples for SEM analysis, the leached blocks and an unleached control block were cut in half widthways under water using a diamond saw and the resultant ~1 cm^3 blocks were set into epoxy resin. The surface to be examined was then polished using water-free diamond paste removing the top 1-2 mm of material potentially exposed to water during cutting. The samples were then carbon coated (~10nm) and backscatter electron images were collected on a FEI Quanta 650 FEGESEM environmental Scanning Electron Microscope (SEM) equipped with an Oxford Instruments INCA 350 Energy-dispersive X-ray spectroscopy system that had an 80mm X-Max Silicon drift detector. Backscattered electrons are incident electrons which have been scattered by the nuclei of atoms within the sample prior to re-emerging from the surface. Since heavier elements produce a stronger backscattering effect, images formed from backscattered electrons provide phase composition detail with phases containing higher atomic mass elements producing a brighter image.

Energy-dispersive X-ray spectroscopy (EDS) mapping and quantitative point analysis were processed using the Oxford Instruments AZtec acquisition and analysis software. EDS uses the incident electron beam of the SEM as an excitation source to elevate core electrons from their orbitals. When a valence electron falls to fill the core hole, energy is released as characteristic x-rays which are detected by the silicon drift detector (all elements from the atomic mass of C upwards can be detected). The energies of these x-rays vary systematically by element with generally minimal overlap of peaks allowing both rapid 'fingerprinting' of the chemical composition of a sample or semi-quantitative analysis when data is collected under controlled geometry and a calibration standard is used. False colour SEM-EDS elemental maps were used to identify phases, and phase composition was subsequently determined both near and remote from the leached surface of each slag block by point counting using randomly oriented 20x20μm grids [1]; (e.g. SI Fig. S1a). EDS was also used to quantify phase composition in selected V-containing BOF slag phases. Multiple EDS spot analyses (analysis volume of 2 μm^3; working distance, 10 mm) were collected and elemental

composition was determined using the AZtec software (a Co metal target was used as the calibration standard and regular recalibration was undertaken to prevent drift in total detector counts between analyses).
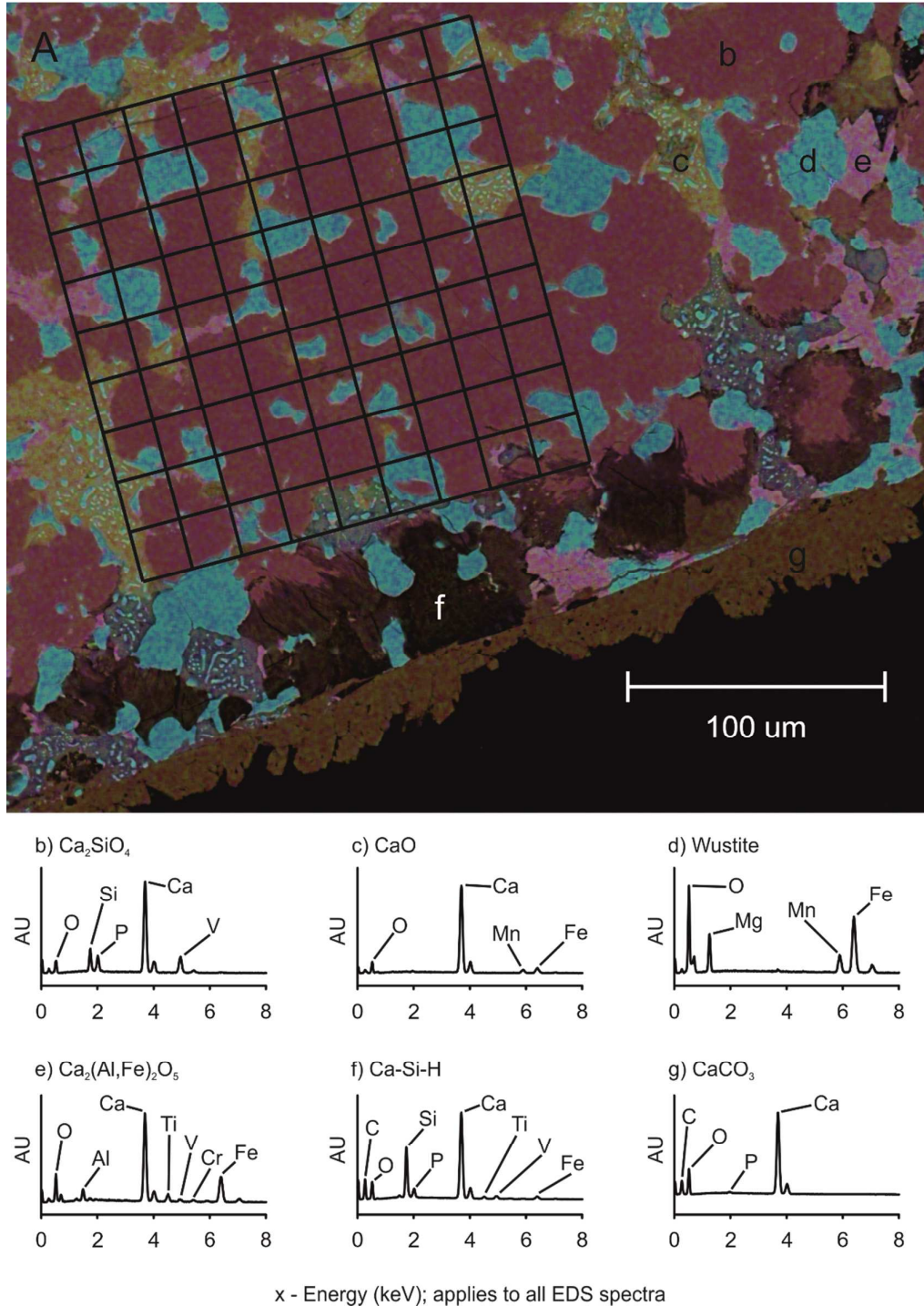

Figure S1. A) Example composite false colour SEM-EDS elemental maps showing phase discrimination within the BOF slag samples and location of typical randomly orientated 20 x 20 μm grid used to determine phase concentrations (v/v) within the bulk slag and weathered regions. Data

from several locations and maps were used to allow for averaging of micron-scale heterogeneity in phase composition. b-g) Example EDS spectra collected from each of the 6 major phases detected.

Section S2. XAS analysis.

Polished BOF slag blocks were produced from samples recovered from both the aerated, air-excluded leaching experiments and from identical unweathered samples. Standard materials (V_2O_5; $VOSO_4$) were also prepared as pressed pellets using cellulose as a diluent to reduce chemical thickness (to achieve an edge step between 0.5 and 1.5 in transmission mode, see below). Pellets were held in Kapton™ tape. A sodium vanadate solution was prepared in 0.1 mol.L^{-1} NaOH, also at 1000 mg.L^{-1}, and held in a polythene bag.

μXAS spectra and μ XRF maps were collected at the V K-edges (5465 eV) on beamline I18 at the Diamond Light Source operating at 3 GeV with a typical current of 250 mA, using a nitrogen cooled Si(111) double crystal monochromator and focussing optics. A pair of plane mirrors was used to reduce the harmonic content of the beam and Kirkpatrick-Baez mirrors were used to produce a focused beam (approximately 2μm diameter at the sample). For standards prepared as pressed pellets, K-edge spectra were collected in transmission mode at room temperature (~295 °K). For samples and solutions, data were collected in fluorescence mode using a 9 element solid state Ge detector at room temperature.

μXRF elemental maps were collected for selected regions within the slag blocks (~150 x 100 pixels; 2 μm^2 per pixel) for Ca, Ti, V, Cr, Mn and Fe. Each individual pixel in the maps could be interrogated by the acquisition software to produce a XRF spectra that could be compared to SEM-EDS spectra collected previously from slag phases. A combination of the μXRF maps, XRF spectra and position within the sample was used to identify specific points of interest within the sample for μXANES analysis as shown in Figure S2. Multiple scans (n = 5-9; k = 0-8 $Å^{-1}$) were averaged to improve the signal to noise ratio using Athena version v0.9.24 [2]. The step size was 0.3 eV over the XANES region (-50 – 100 eV) and 3-5 eV in the pre- and post-edge regions. For μXANES spectra absorption was normalised in Athena over the full data range and plotted from approximately -20 eV to +40 eV relative to the edge position with no correction required for drift in E_0. V data was calibrated using E_0 measured from thin metal foils.
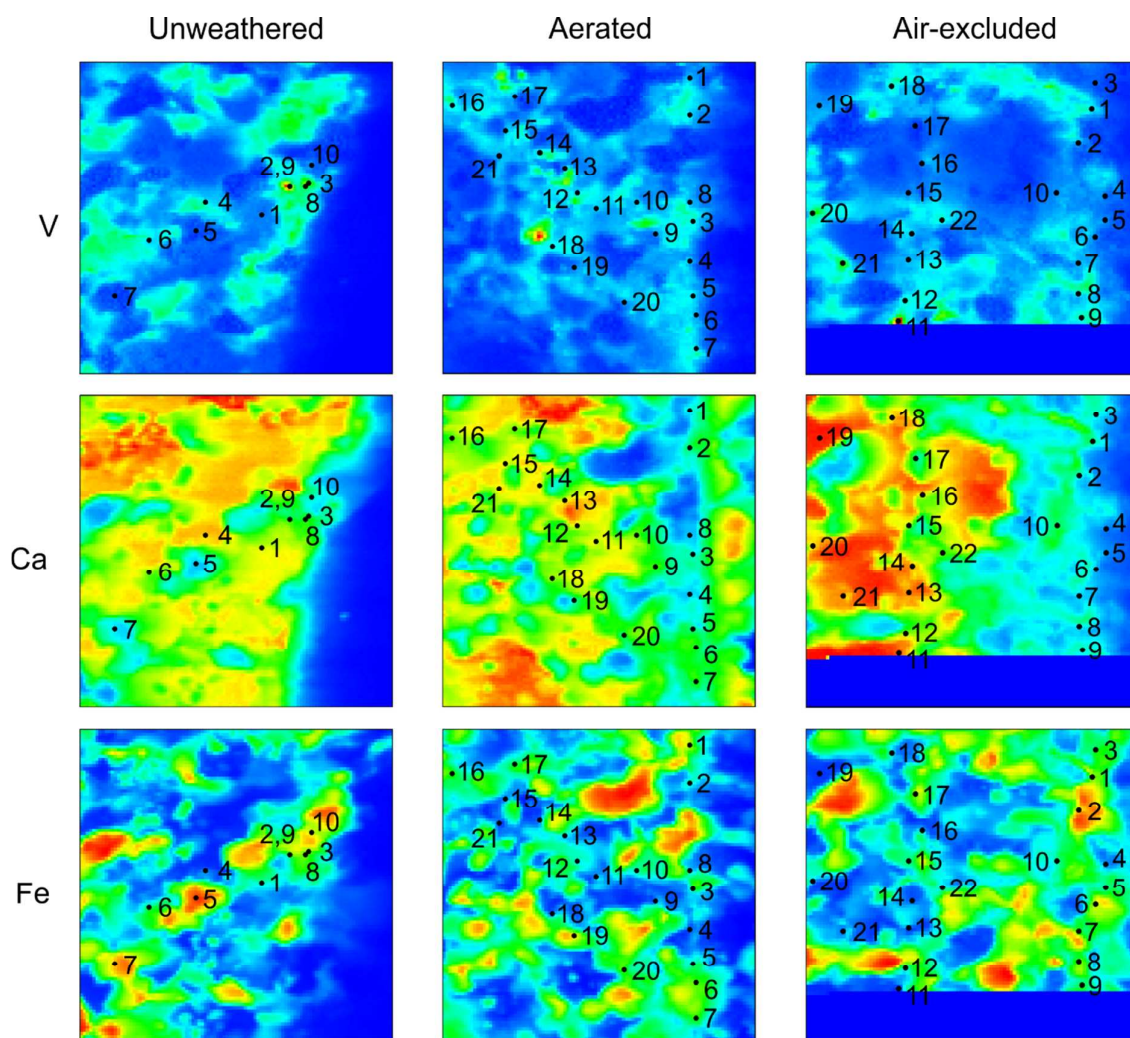
Figure S2. V, Ca and Fe μXRF maps collected from the slag blocks recovered from the aerated, air-excluded leaching experiments and from an unweathered sample; numbered points indicate locations where μXANES spectra were collected.

In general, XAS involves application of x-rays to a sample with an energy at or just above the binding energy of core electrons of a specific element to promote excitation of electrons to higher orbitals. K-edge spectra are produced during electron transitions from the lowest (1s) electron orbitals. Typical features of V K-edge XAS spectra are shown in Figure S3.
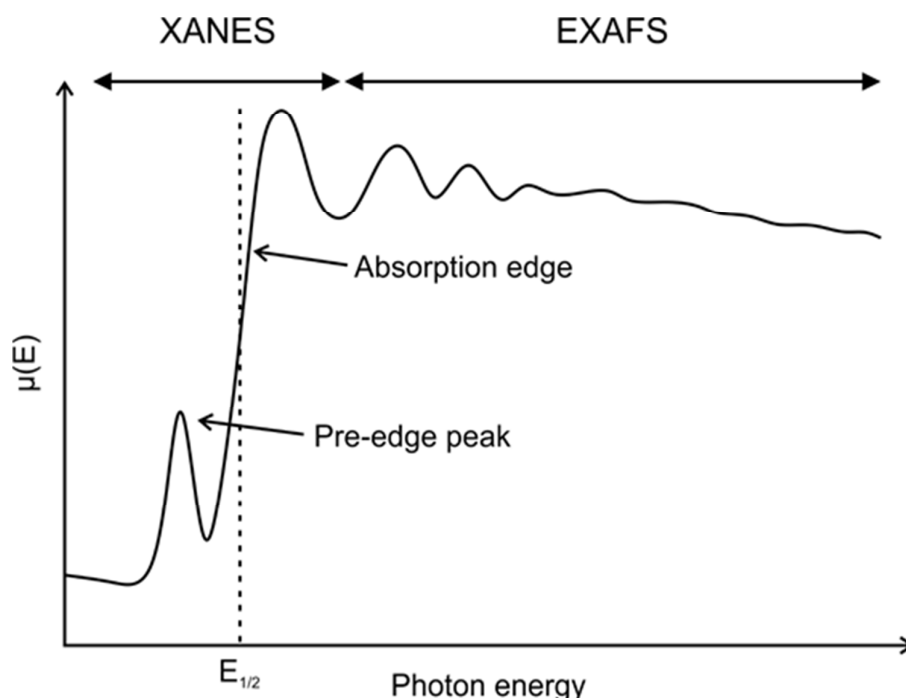
Figure S3. Typical features associated with V-Kedge XAS spectra.

The pre-edge peak is formed during electron transitions to unoccupied bound states. These transitions are constrained by dipole selection rules and so 1s electrons must end up in a p-like final state. The p-levels of transition metal oxides are often filled, however, under certain conditions full p-orbitals may be hybridised with unfilled d-orbitals, thus allowing these transitions to take place. Pre-edge peaks in V XANES spectra are dependent on 1s transitions to hybridised 3d/4p orbitals which readily occur in tetrahedral coordination resulting in a prominent pre-edge peak. The effect of hybridisation is reduced in square pyramidal coordination and again in octahedral coordination leading to correspondingly smaller pre-edge peaks. The absorption edge represents electron transitions to continuum states. The position of the edge (defined as energy at 0.5 of the normalised edge step i.e. $E_{1/2}$) generally moves to higher energies with increasing valence due to the increased binding energies caused by the decrease in electron numbers.

A robust method for determining V speciation and coordination symmetry from XANES spectra has been developed by Charaund et al [3]. They found that the position of the absorption edge alone is not sufficient to determine the oxidation state of V as it can overlap more than one

valence state (e.g. V^{3+} and V^{4+} are not well resolved using this method). Similarly, pre-edge peak intensity cannot be relied upon due to a considerable overlap between V^{4+} in square pyramidal coordination and V^{5+} in octahedral or square pyramidal coordination. Detailed examination of both can resolve both coordination symmetry and oxidation state of V^{3+}, V^{4+} and V^{5+}.
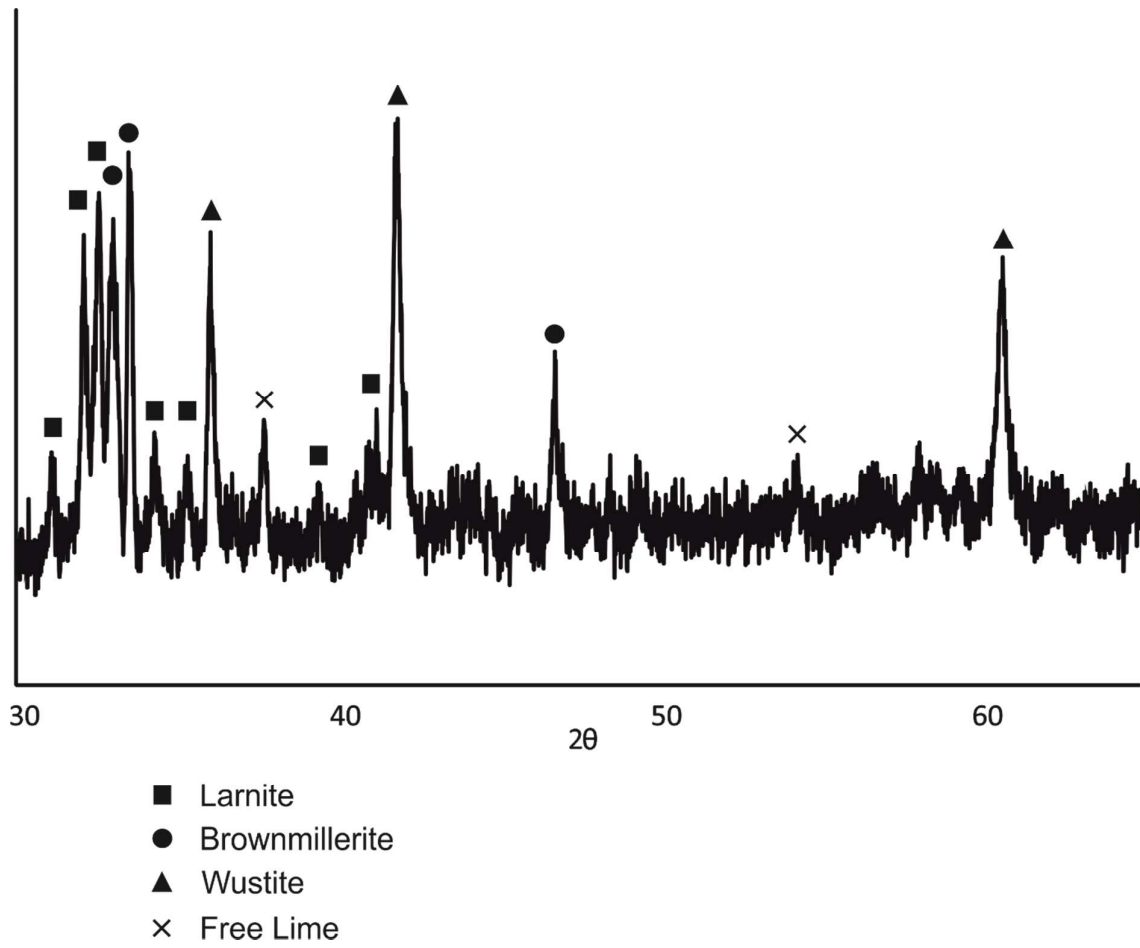
Figure S4. XRD pattern collected from the crushed steel slag sample annotated with major phase peaks detected.
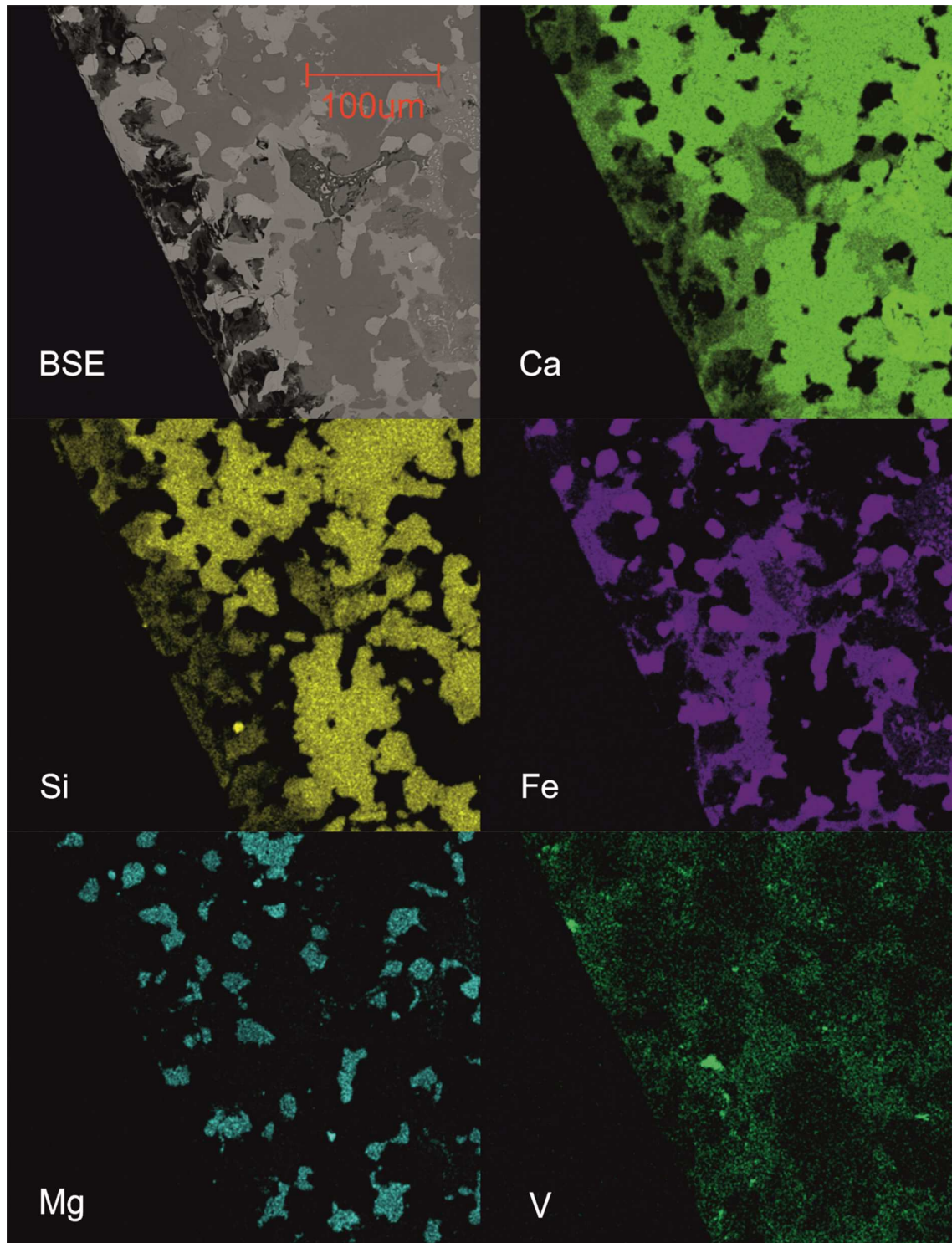
Figure S5 Slag surface structure after 6 months weathering under air-excluded conditions; backscatter electron image and false colour EDS element maps.
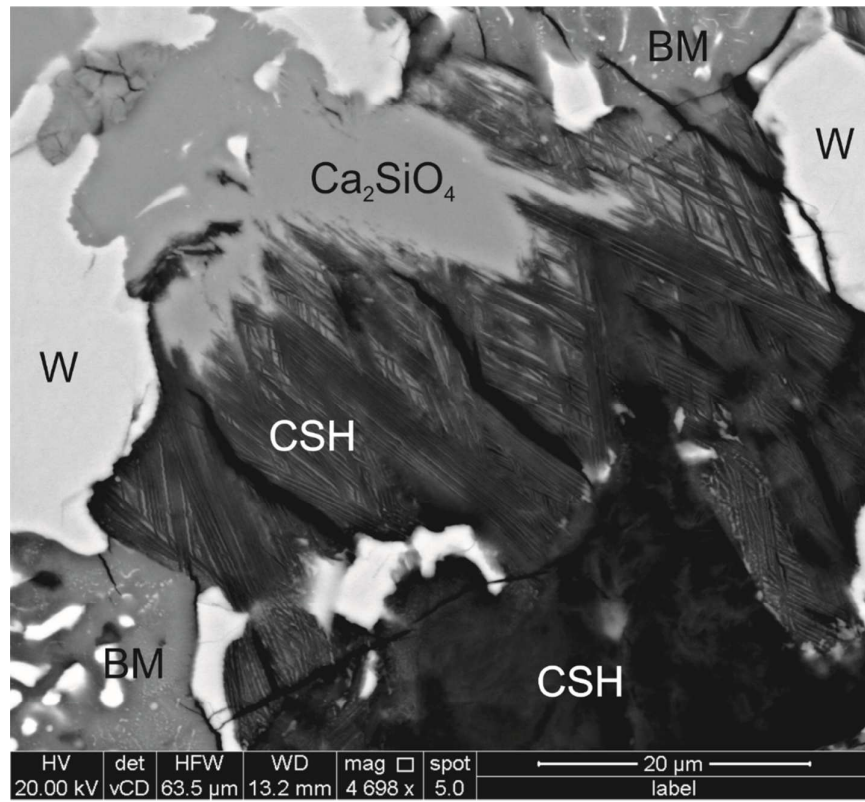
Figure S6 Backscattered electron image showing an example altered region where Ca-Si-H is replacing dicalcium silicate.

Table S1. Mean (± 1 standard deviation) chemical composition determined for set of 21 BOF Steel slag samples collected from Yarborough, UK. Data is presented in both nominal oxide and elemental composition formats. Uncertainty (versus certified standards) was < ±30% for Mg, < ±20% for S and, < ±10% for all other elements.

Nominal Oxide Composition*	Oxide Weight %	Elemental Composition	Weight %	Elemental Limit of Detection
CaO	40 ±5.4	Ca	29 ±3.9	<0.05
FeO	32 ±9.4	Fe	25 ±7.3	<0.001
SiO_2	14 ±3.4	Si	6.5 ±1.6	<0.1
MgO	5.2 ±1.1	Mg	3.1 ±0.7	<0.5
MnO	4.5 ±0.8	Mn	3.5 ±0.6	<0.001
Al_2O_3	1.2 ±0.4	Al	0.71 ±0.24	<0.2
P_2O_5	1.3 ±0.4	P	0.57 ±0.17	<0.05
V_2O_5	0.81 ±0.24	V	0.45 ±0.13	<0.001
TiO_2	0.30 ±0.13	Ti	0.18 ±0.08	<0.001
Cr_2O_3	0.24 ±0.13	Cr	0.16 ±0.08	<0.001
SO_3	0.23 ±0.09	S	0.09 ±0.04	<0.02

*It is a very common practice in geoscience and materials science to present XRF data as a set of nominal oxide phases. This allows calculation of the total % oxides present as a simple check on quality control (a totals oxide percentage close to 100% implies that no major elements are missing and that the calibration method was successful). However, this convention does not imply that these simple oxide phases are actually present in the samples as no speciation data is provided by the analysis.

Table S2. Average of quantitative SEM-EDS spot analysis collected from selected primary and secondary phases within the BOF slag samples. LoD typically = 0.1 wt% for most elements. C is not determined in the analysis and element totals less than 100 % are, therefore, due to the inclusion of C-based resin (which also contains S and Cl) in the sample volume (~2 μm^3); or in the case of the $CaCO_3$ phase, C within the carbonate moiety itself.

Element	Ca_2SiO_4 (wt%; n=11)	$Ca_2(AlFe)_2O_5$ (wt%; n=17)	Ca-Si-H (wt%; n=23)	$CaCO_3$ (wt%; n=1)
O	37.9 ±1.6	31.3 ±2.6	21.2 ±9.7	48.7
Mg	n.d.	0.49 ±0.09	0.08 ±0.05	n.d.
Al	0.16 ±0.06	3.1 ±0.4	0.33 ±0.19	n.d.
Si	13.2 ±0.7	0.50 ±0.14	4.7 ±2.2	n.d.
P	1.5 ±0.1	n.d.	2.5 ±1.0	0.17
S	n.d.	n.d.	0.10 ± 0.10	n.d.
Cl	n.d.	n.d.	0.15 ±0.11	n.d.
Ca	41.5 ±1.5	28.2 ±2.5	13.9 ±5.8	40.4
Ti	0.21 ±0.09	3.2 ±0.8	0.60 ±0.29	n.d.
V	0.44 ±0.23	1.14 ±0.14	0.70 ±0.57	n.d.
Cr	n.d.	0.42 ±0.14	0.06 ±0.01	n.d.
Mn	n.d.	0.81±0.0.8	0.18 ±0.16	n.d.
Fe	0.81 ±0.09	24.9 ±2.3	1.9 ±0.8	n.d.
TOTAL	*95.7 ±3.4*	*94.1 ±8.0*	*44.2 ±18.7*	*89.3*

n.d. = not detected; n =number of data points

References

1.   Plas, L.v.d. and A.C. Tobi, *A chart for judging the reliability of point counting results.* American Journal of Science, 1965. **263**(1): p. 87-90.
2.   Ravel, B. and M. Newville, *ATHENA, ARTEMIS, HEPHAESTUS: data analysis for X-ray absorption spectroscopy using IFEFFIT.* J Synchrotron Radiat, 2005. **12**(Pt 4): p. 537-41.
3.   Chaurand, P., et al., *New methodological approach for the vanadium K-edge X-ray absorption near-edge structure interpretation: Application to the speciation of vanadium in oxide phases from steel slag.* Journal of Physical Chemistry B, 2007. **111**(19): p. 5101-5110.